CHINESE OPTICS LETTERS

Vol. 20, No. 9 | September 2022

White light interferometry with spectral-temporal demodulation for large-range thickness measurement

Yunlong Zhu (朱云龙)[1,2], Zhuoran Li (李卓然)[1,2], Xu Lu (卢 旭)[1,2], Yonggui Yuan (苑勇贵)[1,2*], and Jun Yang (杨 军)[2,3,4**]

[1] Key Laboratory of In-fiber Integrated Optics, Ministry of Education of China, Harbin Engineering University, Harbin 150001, China

[2] College of Physics and Optoelectronic Engineering, Harbin Engineering University, Harbin 150001, China

[3] Guangdong Provincial Key Laboratory of Information Photonics Technology (Guangdong University of Technology), Guangzhou 510006, China

[4] School of Information Engineering, Guangdong University of Technology, Guangzhou 510008, China

*Corresponding author: yuanyonggui@aliyun.com

**Corresponding author: yangj@gdut.edu.cn

Received February 2, 2022 | Accepted May 17, 2022 | Posted Online June 12, 2022

Film thickness measurement can be realized using white light interferometry, but it is challenging to guarantee high precision in a large range of thicknesses. Based on scanning white light interferometry, we propose a spectral-temporal demodulation scheme for large-range thickness measurement. The demodulation process remains unchanged for either coatings or substrate-free films, while some adjustments are made according to the estimated optical thickness. Experiments show that the single-point repeatabilities for 500 nm SiO_2 coating and 68 μm substrate-free Si film are no more than 0.70 nm and 1.22 nm, respectively. This method can be further developed for simultaneous measurement of surface profile and film thickness.

Keywords: white light interferometry; thickness measurement; spectral-temporal demodulation; thin film.
DOI: 10.3788/COL202220.091201

1. Introduction

Thin films play important roles in the fields of semiconductors, optoelectronics, integrated optics, etc. Following the increasing demand on thin film quality[1], precise measurement of film thickness is crucial to provide valuable feedback for the fabrication process. While dealing with transparent thin films, commercial ellipsometry systems[2] can give good results of film thickness, yet they can hardly measure surface profile and film thickness at the same time. On the contrary, white light interferometry (WLI) is well-known for surface profile measurement with high precision, and it shows great potential for simultaneous measurement of film thickness and surface profile[3], yet it is hard to measure a large range of thickness with high accuracy.

The measurement of film thickness using WLI can be realized through time-domain detection[4–9] or spectral-domain detection[3,10–13]. For WLI with time-domain detection, the interferometric signal is obtained by temporal scanning of the optical path difference (OPD), and the signal will contain two peaks corresponding to the reflection from the front and rear surfaces of the thin film. Film thickness can be obtained by calculating the distance between these peaks. However, when the optical thickness of film is less than the coherence length of the white light source, these two peaks are mixed with each other, which affects the precision of thickness measurement. In this case, it is feasible to measure the thickness by building and solving nonlinear equations or by applying model-based fitting methods, yet the phase change with reflection and the multi-reflection in thin film should be carefully dealt with for high-precision measurements[4,9,14]. For WLI with spectral-domain detection, the interferometric signal is obtained using a spectrometer. By analyzing the reflectance spectrum from thin film, the thickness can be determined[3,10–12]. It is suitable for the measurement of thin film with small optical thickness (less than the coherence length of light source), but the range of measurable thickness is limited by the parameters of the spectrometer, while the application of a high-performance interferometer will significantly increase the cost of the measuring system.

Since the Fourier transform of the time-domain interferometric signal is equivalent to the spectrum when the numerical aperture (NA) is approximately equal to zero[15], which is the principle of Fourier transform infrared (FTIR) spectroscopy, it is also feasible to apply spectral demodulation methods using time-domain detection. Thin films with thickness from 50 nm to 1.5 μm can be measured using this demodulation scheme[5–8]. Besides, the spectral phase information obtained by Fourier transform can also be applied to demodulate the value of thickness[15]. Yet, the upper limit of measurable thickness is still relatively small.

In this paper, we propose a spectral-temporal demodulation method to realize high-precision thickness measurement in a large range of thicknesses. The theoretical full-range precision and lower limit of thickness are determined by the spectral demodulation method, and the theoretical upper limit of thickness is determined by the scanning range of the optical delay line. A home-made fiber-optic scanning WLI with gradient-index (GRIN) lens probe[16] is applied. A weak reflector is inserted in the probe to provide reference. Five-point thickness measurements for a coating of SiO_2 (thickness ≈ 500 nm) on Si as well as a substrate-free Si film (thickness ≈ 68 μm) are realized using the proposed method. This method can be easily extended to simultaneous measurement of film thickness and surface profile by applying collimated illumination and a two-dimensional detector, since the absolute position information is also contained in the interferometric signal.

2. Principle

In this paper, we use scanning WLI to realize thickness measurement of transparent coating or substrate-free film with a large thickness range. A home-made WLI system[16] with double probes is applied, yet one probe is enough for the thickness measurement of transparent films, which is discussed in this paper. It is a fiber-based system for single-point measurements, and the NA is approximately equal to zero. The probe follows the design described in Ref. [16] with a weak reflection surface inside. A broad-spectrum light source is applied, and the incident light field E_0 can be described as

$$E_0(k) = A_0(k)e^{i\theta(k)}, \tag{1}$$

where k is the wave number, A_0 is the amplitude representing the spectral distribution of the light source, and θ is the initial phase.

The reflected light field E_1 from the reflecting surface and the film under test can be expressed as

$$E_1(k) = r_p(k)E_0(k) + (1 - r_p^2(k))r(k)E_0(k)e^{ikL}, \tag{2}$$

where r_p and r are the Fresnel reflection coefficients of the reflecting surface and film under test, respectively, and L is two times the distance between the reflecting surface and the surface of the thin film.

For coatings (without reflection from the backside of the substrate) and substrate-free films, the refractive index of the film under test is set to be n_1, and the refractive index of the substrate (or air for substrate-free films) is set to be n_2. We define d as the thickness of film; thus the reflectance of the coating R can be expressed as follows:

$$R(k) = |r(k)|^2, \tag{3}$$

with

$$r(k) = \frac{r_1(k) + r_2(k)e^{-2ikn_1(k)d}}{1 + r_1(k)r_2(k)e^{-2ikn_1(k)d}}, \tag{4}$$

where r_1 and r_2 are defined as

$$r_1(k) = \frac{1 - n_1(k)}{1 + n_1(k)}, \tag{5}$$

$$r_2(k) = \frac{n_1(k) - n_2(k)}{n_1(k) + n_2(k)}. \tag{6}$$

Also, the reflectance R_p and the transmittance T_p of the probe are expressed as follows:

$$R_p(k) = |r_p(k)|^2 = r_p^2(k), \tag{7}$$

$$T_p(k) = 1 - R_p(k) = 1 - r_p^2(k). \tag{8}$$

In the scanning WLI, the light is divided into two beams after passing through the coupler. After passing through the optical delay line, the two beams interfere with each other, and the total light field E is

$$\begin{aligned} E(k,S) &= q_1E_1(k) + q_2E_1(k)e^{ikS} \\ &= E_0(k)(r_p + T_p(k)r(k)e^{ikL})(q_1 + q_2e^{ikS}), \end{aligned} \tag{9}$$

where q_1 and q_2 are two intensity coefficients of the two beams, respectively, and S is the OPD between two beams introduced by the optical delay line. The interferometric signal I is expressed as

$$\begin{aligned} I(S) &= \sum_k |E(k,S)|^2 \\ &= \sum_k A_0^2(k)|r_p(k)q_1 + r_p(k)q_2e^{ikS} + T_p(k)|r(k)|q_1e^{ikL+i\varphi(k)} \\ &\quad + T_p(k)|r(k)|q_2e^{ik(L+S)+i\varphi(k)}|^2, \end{aligned} \tag{10}$$

where φ is the phase deviation introduced by the thin film. Since differential detection is used to filter out the DC term, the interferometric signal I_f we finally get is

$$I_f(S) = 4q_1q_2\sum_k A_0^2(k)(U_1(k) + U_2(k) + U_3(k)), \tag{11}$$

with

$$U_1(k) = (R_p(k) + T_p^2(k)R(k))\cos\, kS, \tag{12}$$

$$U_2(k) = r_p(k)T_p(k)|r(k)|\cos(k(L + S) + \varphi(k)), \tag{13}$$

$$U_3(k) = r_p(k)T_p(k)|r(k)|\cos(k(L - S) + \varphi(k)). \tag{14}$$

It can be seen from Eqs. (11)–(14) that due to the low coherence of the broad-spectrum light source, there are three peaks in the interferometric signal (around $S = 0$, L, $-L$, respectively). By demodulating the distance between these peaks, we can obtain L, which means the profile of the thin film surface can be obtained with two-dimensional detection. Since only single-point

detection is applied in our experiments, the demodulation of L is not discussed in this paper.

This scanning process is actually equivalent to FTIR measurement of E_1. The time-domain interference signal is the Fourier transform of the spectral signal, and vice versa. In the time domain, we can easily separate the interferometric signal around the central peak ($S \approx 0$) to obtain the spectrum $F(k)$:

$$F(k) = 4q_1 q_2 A_0^2(k)(R_p(k) + T_p^2(k)R(k)). \tag{15}$$

This step has the same intention of applying a "spectral carrier" described in Ref. [3], yet we take only one Fourier transform instead of two, since the time-domain signal is directly taken.

Without film under test, the reflectance spectrum of the reflecting surface in probe F_p to be measured is

$$F_p(k) = 4q_1 q_2 A_0^2(k)R_p(k). \tag{16}$$

When testing a reference surface with known reflectance R_{ref}, the reference spectral F_{ref} can be obtained:

$$F_{\text{ref}}(k) = 4q_1 q_2 A_0^2(k)(R_p(k) + T_p^2(k)R_{\text{ref}}(k)), \tag{17}$$

with

$$R_{\text{ref}}(k) = |r_{\text{ref}}(k)|^2 = \left(\frac{1 - n_{\text{ref}}(k)}{1 + n_{\text{ref}}(k)}\right)^2. \tag{18}$$

According to Eqs. (15)–(18), the reflectance spectrum R can be obtained:

$$R(k) = \frac{F(k) - F_p(k)}{F_{\text{ref}}(k) - F_p(k)} R_{\text{ref}}(k). \tag{19}$$

The film thickness can be obtained by fitting $R(k)$ to the theoretical curve described by Eqs. (3)–(6). The sum of squared errors W is described as

$$W(d_{\text{in}}) = \sum_k |R_{\text{th}}(d_{\text{in}},k) - R(k)|^2, \tag{20}$$

where R_{th} is the theoretical value of R with input thickness d_{in}.

The Levenberg–Marquardt (LM) algorithm[17] is applied to obtain the demodulated thickness, which theoretically corresponds to the minimum value of W. To obtain correct results using the LM algorithm, proper initial values are needed. For nano-scale thin films, the film thickness can be roughly estimated according to the parameters of fabrication process, and the absolute error is generally no more than 100 nm. Thus, the estimated thickness can be used as the initial value for the LM algorithm. However, for films with larger thickness, the absolute error of estimated thickness can be large, even with the same scale of relative error. According to Eqs. (3), (4), and (20), whenever the value of optical thickness changes by about half the center wavelength of the light source, a local minimum value of W will occur. The thickness difference Δd between the local minima of W can be expressed as

$$\Delta d \approx \frac{\lambda_c}{2n_g(\lambda_c)}, \tag{21}$$

where λ_c is the center wavelength of the light source, and n_g is the group index. If we still take the estimated thickness as the initial value for the LM algorithm, the output often takes the nearest local minimum point, which brings errors to the thickness measurement.

However, for a film with a large thickness, the OPD between the front and back is usually much larger than the coherence length of the white light source. Therefore, the rough value of film thickness d_0 can be obtained in the time-domain interferometric signal by the envelope method[18]. d_0 is usually much more precise than the thickness estimated by the manufacturer, yet errors larger than Δd may still occur. To make sure that we have a proper initial value for the LM algorithm, we take a set of initial values d_{ini} defined as

$$d_{\text{ini}} = d_0 \pm m\Delta d, \tag{22}$$

where practically we take $m = 0, 1, 2, 3$. Accordingly, the LM algorithm is carried out seven times using different initial values. Among the seven results, the one with the minimum sum of squared errors is taken as the measured thickness value.

We should also pay attention to another issue concerning the fitting process. $R(k)$ oscillates with higher frequency in the spectral domain while dealing with larger thicknesses. In this case, phase error may occur in the spectral signal[19], which may also bring errors for the fitting process. To solve this problem, we perform Hilbert transform on the theoretical and the measured R, respectively, and take the argument to get the phase signal α:

$$\alpha(k) = \arg(\text{Hilbert}(R(k))). \tag{23}$$

Theoretically, the obtained phase α can be used for the fitting process. However, α is a wrapped phase signal, which means the phase ambiguity of the integer multiple of 2π exists. Although α can be unwrapped with the proper algorithm, which avoids the phase jump around 0 and 2π, the integer multiple of 2π may still exist between measured and theoretical values of α. For this reason, additional preprocessing is needed before the fitting of α, which will increase the algorithmic complexity. Besides, incorrect unwrapped values of α and the deviation of α at few points tend to cause relatively large error when a direct fitting of unwrapped α is carried out. In order to get more reliable fitting results with a simpler process, we define signal β as

$$\beta(k) = \cos(\alpha(k)). \tag{24}$$

β contains the phase information of α, and the sudden jumps caused by phase wrapping in α are also avoided. Although the cosine function may change the frequency distribution of noise, experimental results show that the influence is negligible. So, for

the simplicity and reliability of the thickness demodulation process, we fit β instead of R while measuring large thickness.

3. Experimental Results

In the experiments, the center wavelength of the white light source is 1310 nm, and the full width at half-maximum of the spectrum is about 70 nm. In order to verify the reliability of the proposed method, a 500 nm SiO_2 coating on the Si substrate and a 68 μm substrate-free film were selected for thickness measurement. The back surface of the Si substrate for SiO_2 coating is a highly scattering surface, so the reflection can be ignored although Si is transparent to the 1310 nm light source. The optical thickness of the SiO_2 coating is smaller than the coherence length of the light source, so the peaks caused by different surfaces of the thin film overlap with each other. On the contrary, the optical thickness of the Si film is greater than the coherence length, so the peaks caused by different surfaces of thin film can be distinguished. To measure the thickness and uniformity of the films, classical five-point measurement was carried out for each film, and five repeated measurements were performed at each point.

According to Eq. (19), F, F_p, F_{ref}, and R_{ref} need to be known to calculate R. In our experiments, F is measured using the film under test (SiO_2 coating or substrate-free Si film), F_p is measured without any film facing the probe, F_{ref} is measured using a bare Si wafer with a polished front surface and highly scattering back surface, and R_{ref} is calculated according to the refractive index of Si. Since the fluctuation of ambient temperature may have an influence on the measurements, the measurements are preferred to be carried out with the minimum time interval.

For the measurement of 500 nm SiO_2 coating, $F(k)$, $F_{\mathrm{ref}}(k)$, and $F_p(k)$ for one of the measurements are shown in Fig. 1(a). Least squares fitting is carried out directly with the reflectance spectrum $R(k)$. The initial value for the LM algorithm is directly set to be 500 nm. The experimental and theoretical curves of $R(k)$ are shown in Fig. 1(b), where the value of thickness for the calculation of the theoretical curve is the result given by the LM algorithm. The complete measurement results are shown in Table 1. Among the five points, the maximum single-point standard deviation is 0.70 nm. It can also be calculated that the average thickness of the film is 509.35 nm, and the standard deviation between the five points is 2.57 nm.

To test the correctness of the fitting process, the sums of squared errors with d_{in} ranging from 0 to 1000 nm are plotted in Fig. 1(c), while Fig. 1(d) is a detailed view showing more clearly the points of local minima. It can be seen that the minimum around 509.35 nm is truly the minimum among all the minima in this range. Besides, the nearest local minimum is about 100 nm away, so the value of 500 nm given by the manufacturer works well as the initial value for the LM algorithm.

For the measurement of 68 μm Si film, $F(k)$, F_{ref} (k), and $F_p(k)$ for one of the measurements are shown in Fig. 2(a). Since the thickness is relatively large, least squares fitting is carried out with $\beta(k)$ described by Eq. (24). To get the proper initial values for the LM algorithm, the traditional envelope method is applied to give the values of d_0, as shown by Table 1. For 68 μm Si film and 1310 nm light source, Δd in Eq. (21) is estimated to be 0.18 μm. The values of d_{ini} in Eq. (22) are then taken as the initial values for the LM algorithm. As discussed in Section 2, seven results of thickness measurements are thus given for each measurement, and the final result is chosen to be the one with the minimum sum of squared errors.

The experimental and theoretical curves of $\beta(k)$ are shown in Fig. 2(b), where the value of thickness for the calculation of the theoretical curve is the final result given by the LM algorithm. The complete measurement results given by envelope method and the proposed method are shown in Tables 2 and 3, respectively. Among the five points, the maximum single-point standard deviation is 1.2 nm for the proposed method, while this value is 26 nm for the envelope method. By comparing the values of standard deviation in Tables 2 and 3, we can see that the

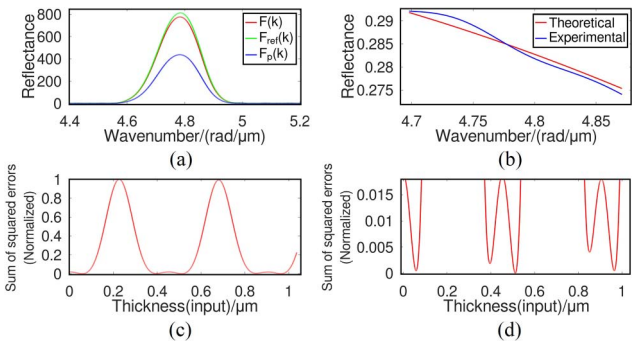

Fig. 1. Experimental results for a single measurement of 500 nm SiO_2 coating. (a) Reflectance spectrum $F(k)$, $F_{\mathrm{ref}}(k)$, and $F_p(k)$. (b) Comparison of measured reflectance $R(k)$ and theoretical model. (c) Normalized sum of squared errors for reflectance fitting between the experimental result and theoretical model at different values of input thickness. (d) Detailed view of (c) showing the minimum sum of squared errors.

Table 1. Measurement Results for 500 nm SiO_2 Coating (nm).

Number of Measurement	Point A	Point B	Point C	Point D	Point E
1st	508.18	511.34	506.86	508.84	513.53
2nd	508.67	511.09	505.66	508.62	512.71
3rd	507.31	511.60	506.88	508.98	512.03
4th	507.65	511.36	506.52	508.26	512.81
5th	508.00	511.53	506.03	507.23	512.07
Average	507.96	511.38	506.39	508.39	512.63
Standard deviation	0.52	0.20	0.53	0.70	0.62

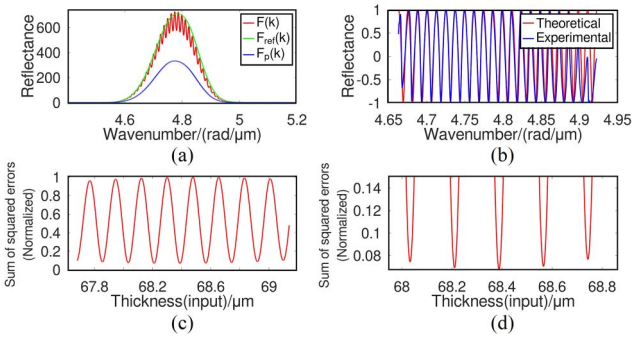

Fig. 2. Experimental results for a single measurement of 68 μm Si film. (a) Reflectance spectrum $F(k)$, $F_{\mathrm{ref}}(k)$, and $F_p(k)$. (b) Comparison of measured reflectance $R(k)$ and theoretical model. (c) Normalized sum of squared errors for reflectance fitting between the experimental result and theoretical model at different values of input thickness. (d) Detailed view of (c) showing the minimum sum of squared errors.

Table 2. Measurement Results for 68 μm Si Film Using Envelope Method (nm).

Number of Measurement	Point A	Point B	Point C	Point D	Point E
1st	68,613.59	68,348.37	68,394.21	68,299.25	68,554.65
2nd	68,646.33	68,345.09	68,364.74	68,243.59	68,528.46
3rd	68,613.59	68,322.17	68,387.66	68,282.88	68,557.92
4th	68,643.06	68,341.82	68,404.03	68,276.33	68,535.00
5th	68,597.22	68,358.19	68,390.93	68,295.98	68,593.94
Average	68,622.76	68,343.13	68,388.31	68,279.61	68,554.00
Standard deviation	21	13	15	22	26

Table 3. Measurement Results for 68 μm Si Film Using the Proposed Method (nm).

Number of Measurement	Point A	Point B	Point C	Point D	Point E
1st	68,628.97	68,358.91	68,387.23	68,330.20	68,563.33
2nd	68,628.64	68,358.97	68,387.58	68,331.68	68,563.89
3rd	68,629.01	68,359.5	68,388.33	68,332.76	68,564.37
4th	68,628.80	68,359.38	68,388.35	68,332.86	68,564.22
5th	68,629.03	68,359.58	68,388.68	68,333.17	68,564.56
Average	68,628.89	68,359.27	68,388.04	68,332.13	68,564.07
Standard deviation	0.17	0.31	0.60	1.2	0.48

Table 4. Summary of Measurement Uncertainty Components.

Uncertainty Component	Source	Uncertainty Contribution
$u(l_H)$	Measurement results	0.31 nm (see Table 1)
		11.63 nm (see Table 2)
		0.54 nm (see Table 3)
$u(l_f)$	Nominal wavelength	4.35×10^{-2} nm
$u(l_T)$	Temperature change	$6.93 \times 10^{-7} H$ (for SiO_2)
		$2.89 \times 10^{-6} H$ (for Si)
$u(l_s)$	Film installation	$2 \times 10^{-9} H$

repeatability has improved for about 30 times using the proposed method. From Table 3, it can also be calculated that the average thickness of the film is 68.45 μm, and the standard deviation between the five points is 0.13 μm.

The sums of squared errors with d_{in} ranging from 67.8 μm to 69.0 μm are plotted in Fig. 2(c), while Fig. 2(d) is a detailed view showing more clearly the points of local minima near 68.45 μm. It can be seen that the minimum around 68.45 μm is truly the minimum among all the minima in this range, and the intervals between the minima are around 177 nm, which is the value of Δd that we derived. Obviously, 68 μm cannot be taken directly as the initial value for the LM algorithm, which will lead to an output of the local minimum around 68 μm, with an error of about $2\Delta d$.

The measurement uncertainty can be divided into repeatability uncertainty $u(l_H)$, nominal laser wavelength uncertainty $u(l_f)$, temperature change uncertainty $u(l_T)$, and film installation uncertainty $u(l_s)$ (see Table 4). The expanded uncertainty of film thickness measurement is 0.63 nm for the 500 nm SiO_2 coating using the proposed method, 23 nm for 68 μm Si film using the envelope method, and 1.2 nm for 68 μm Si film using the proposed method. It can be seen that the expanded uncertainty is below 2 nm for either film using the proposed method. The expanded uncertainty is much smaller than the difference between neighboring minima shown in Figs. 1(d) and 2(d), which proves the reliability of the proposed method.

4. Conclusions

Based on scanning WLI, a spectral-temporal demodulation scheme is proposed. Half of the distance between peaks (if separable) around $S = L$ (or $S = -L$) is taken as the rough value of optical thickness of the thin film, and the Fourier transform of the central peak (around $S = 0$) in the interferometric signal is analyzed to give the precise value of thickness. The proposed method is not only suitable for coatings, but also suitable for substrate-free films. We take a SiO_2 coating (thickness ≈ 500 nm) on a Si substrate and a substrate-free Si film

(thickness ≈ 68 μm) as samples to test the proposed method. By comparing the errors of least square fitting, it is proved experimentally that the outputs converge to the point of minimum error. For the SiO_2 coating and the substrate-free Si film, the results of thickness given by the five-point method are 509.35 nm and 68.45 μm, respectively, while the maximum values of single-point repeatability are 0.70 nm and 1.22 nm, respectively. Compared with the traditional envelope method, the single-point repeatability for the Si film is about 30 times better. We believe the proposed method can be applied for a larger range of thickness, since theoretically the upper limit of thickness is only limited by the optical delay line, while constantly high precision is maintained in the full range. Besides, by applying a collimated beam and two-dimensional detector, our method can be easily extended to carry out simultaneous measurement of surface profile and film thickness.

Acknowledgement

This work was supported by the National Natural Science Foundation of China (Nos. 62005062 and 61975040), the National Science Fund for Distinguished Young Scholars of China (No. 61925501), and the Open Fund of Guangdong Provincial Key Laboratory of Information Photonics Technology (No. GKPT20-02).

References

1. X. Tian, W. Zhou, K. Ren, C. Zhang, X. Liu, G. Xue, J. Duan, X. Cai, X. Hu, Y. Gong, Z. Xie, and S. Zhu, "Effect of dimension variation for second-harmonic generation in lithium niobate on insulator waveguide," Chin. Opt. Lett. **19**, 060015 (2021).
2. Wuhan Eoptics Technology Co. Ltd., "ME-L Mueller matrix ellipsometer," (in Chinese), http://www.eoptics.com.cn/mljztpy/4551.jhtml (August 8, 2021).
3. Y. S. Ghim and S. W. Kim, "Spectrally resolved white-light interferometry for 3D inspection of a thin-film layer structure," Appl. Opt. **48**, 799 (2009).
4. Y. Yang, H. Yan, S. Li, F. Yang, and W. Jin, "Estimation of gyro bias drift due to distributed polarization cross coupling in the fiber coil," Opt. Express **27**, 10247 (2019).
5. H. Yoshino, A. Abbas, P. M. Kaminski, R. Smith, J. M. Walls, and D. Mansfield, "Measurement of thin film interfacial surface roughness by coherence scanning interferometry," J. Appl. Phys. **121**, 105303 (2017).
6. H. Yoshino, R. Smith, J. M. Walls, and D. Mansfield, "The development of thin film metrology by coherence scanning interferometry," Proc. SPIE **9749**, 97490P (2016).
7. H. Yoshino, J. M. Walls, and R. Smith, "Interfacial surface roughness determination by coherence scanning interferometry using noise compensation," Appl. Opt. **56**, 4757 (2017).
8. H. Yoshino, P. M. Kaminski, R. Smith, J. M. Walls, and D. Mansfield, "Refractive index determination by coherence scanning interferometry," Appl. Opt. **55**, 4253 (2016).
9. M. F. Fay and T. Dresel, "Applications of model-based transparent surface films analysis using coherence-scanning interferometry," Opt. Eng. **56**, 111709 (2017).
10. Y. S. Ghim and S. W. Kim, "Fast, precise, tomographic measurements of thin films," Appl. Phys. Lett. **91**, 091903 (2007).
11. Y. S. Ghim, H. G. Rhee, H. S. Yang, and Y. W. Lee, "Thin-film thickness profile measurement using a Mirau-type low-coherence interferometer," Meas. Sci. Technol. **24**, 075002 (2013).
12. K. Xue, J. Wang, Y. Zhao, and Z. Xiao, "Measurement of glass thickness and refractive index based on spectral interference technology," Appl. Opt. **60**, 7983 (2021).
13. Y. Du, H. Yan, Y. Wu, X. Yao, Y. Nie, and B. Shi, "Non-contact thickness measurement for ultra-thin metal foils with differential white light interferometry," Chin. Opt. Lett. **2**, 701 (2004).
14. P. J. de Groot, X. C. de Lega, and M. F. Fay, "Transparent film profiling and analysis by interference microscopy," Proc. SPIE **7064**, 70640I (2008).
15. S. W. Kim and G. H. Kim, "Thickness-profile measurement of transparent thin-film layers by white-light scanning interferometry," Appl. Opt. **38**, 5968 (1999).
16. X. Lu, Y. Yuan, C. Ma, H. Zhu, Y. Zhu, Z. Yu, X. Zhang, F. Jiang, J. Zhang, H. Li, J. Yang, and L. Yuan, "Self-calibrated absolute thickness measurement of opaque specimen based on differential white light interferometry," IEEE Trans. Instrum. Meas. **69**, 2507 (2020).
17. K. Madsen, H. B. Nielsen, and O. Tingleff, "Methods for non-linear least squares problems," https://orbit.dtu.dk/en/publications/methods-for-non-linear-least-squares-problems-2nd-ed (2004).
18. S. S. C. Chim and G. S. Kino, "Three-dimensional image realization in interference microscopy," Appl. Opt. **31**, 2550 (1992).
19. P. Hlubina, D. Ciprian, J. Luňáňek, and M. Lesňák, "Dispersive white-light spectral interferometry with absolute phase retrieval to measure thin film," Opt. Express **14**, 7678 (2006).